Resonant beat wave excitation of terahertz radiation in a magnetized plasma channel

2010 Phys. Scr. 81 045504

(http://iopscience.iop.org/1402-4896/81/4/045504)

IOP PUBLISHING PHYSICA SCRIPTA

Phys. Scr. **81** (2010) 045504 (5pp) doi:10.1088/0031-8949/81/04/045504

Resonant beat wave excitation of terahertz radiation in a magnetized plasma channel

Manish Kumar, Lalita Bhasin and V K Tripathi

Physics Department, Indian Institute of Technology, Delhi 110016, India

E-mail: kumarmanish21@hotmail.com

Received 29 December 2009
Accepted for publication 12 February 2010
Published 19 March 2010
Online at stacks.iop.org/PhysScr/81/045504

Abstract
The nonlinear mixing of two Gaussian laser beams in a magnetized plasma channel to excite a difference frequency terahertz (THz) radiation is investigated. The beat frequency ponderomotive force imparts an oscillatory velocity to electrons that couples with the pre-existing density ripple to produce a nonlinear current driving the THz radiation. The density ripple provides phase synchronism while the axial magnetic field enhances the nonlinear coupling through cyclotron resonance. The THz power scales with the square of density ripple amplitude and inversely with the square of laser frequencies.

PACS numbers: 52.25.Xz, 52.59.Ye

(Some figures in this article are in colour only in the electronic version.)

1. Introduction

Terahertz (THz) radiation generation has attracted much attention in recent years, as these waves have potential applications in biological imaging [1], remote sensing [2], spectroscopy of solids and liquids, chemical and security identification [3] etc. Conventional sources of THz radiation using short pulse lasers in semiconductors and electro-optic crystals are generally limited to energies of the order of μJ per pulse. THz emissions have also been produced from plasmas using energetic electron beams and subpicosecond laser pulses. These include coherent radiation from plasma oscillations driven by ultrashort laser pulses [4], transition radiation of electron beams [5, 6], synchrotron radiation from accelerator electrons [7, 8], Cherenkov wake radiation in magnetized plasmas [9, 10] and emission from laser plasma channels in air [11]. Antonsen *et al* [2] presented a scheme for THz radiation generation that involves the creation of miniature corrugated plasma channels of period $\sim 40\,\mu$m. The channel supports a laser eigenmode with subluminal phase velocity while the radial ponderomotive force due to the mode causes THz radiation generation. Gildenburg and Wedenskii [18] proposed a novel scheme of THz generation where THz power scales linearly with the laser power. A femtosecond laser pulse of intensity $\sim 10^{14}\,\mathrm{W\,cm^{-2}}$ is line focused on a gas through a circular grating–axicon assembly. The pulse tunnel ionizes the gas, forming a thin plasma cylinder. The electrons produced during the laser pulse retain transverse momentum after the pulse is gone and set in transverse oscillations of the plasma cylinder at frequency $\omega \approx \omega_{\mathrm{po}}/\sqrt{2}$. Liu and Tripathi [13] examined the effect of an ambient magnetic field and density ripple on this scheme. The magnetic field provides the frequency tunability while the density ripple controls the angular orientation of the emitted THz radiation. Recent experiments have shown enhanced coherent emission of THz radiation from semiconductor surfaces in the presence of magnetic fields. Mclaughlin *et al* [12] demonstrated a continuous increase in THz electric field with increasing magnetic field up to $B = 8\,\mathrm{T}$.

In this paper, we investigate the beat excitation of THz radiation using Gaussian laser beams co-propagating along the direction of ambient magnetic field in a rippled density plasma channel. The density ripple can be produced by laser machining [14, 15] or using an axicon–circular grating assembly [16]. The lasers impart oscillatory velocity to plasma electrons and exert a ponderomotive force on them at the beat frequency. The ponderomotive force has a transverse component that drives nonlinear current, producing THz radiation. In section 2, we formulate the problem and solve for beat frequency nonlinear current source. In section 3, we solve for THz radiation generation. In section 4, we determine the power of THz radiation. In section 5 a brief discussion of results is given.

2. Beat frequency current density

Consider a rippled density plasma channel, created by a machining prepulse [14, 15] or by a pulse employing a circular grating–axicon assembly [16]. The plasma density can be taken as

$$\begin{aligned} n_o &= n'_o + n'_q, \\ n'_o &= n_o^o\left(1+\frac{r^2}{r_c^2}\right), \\ n'_q &= n_q\left(1+\frac{r^2}{r_c^2}\right)e^{iqz}, \end{aligned} \tag{1}$$

where q is the ripple wave number, r_c is the plasma channel width and the real part of the above equation is implied. The plasma has a static magnetic field $B_s\hat{z}$. Two laser beams with electric fields

$$\vec{E}_j = \vec{A}_j e^{-i(\omega_j t - k_j z)}, \quad j = 1, 2, \tag{2}$$

propagate through the channel with $\omega_j \gg \omega_c = eB_s/mc$, where e and m are the electron charge and mass, ω_c is the electron cyclotron frequency and c is the velocity of light in free space. The amplitudes of the lasers, ignoring the effect of the ripple, are governed by

$$\frac{\partial^2 \vec{A}_j}{\partial r^2} + \frac{1}{r}\frac{\partial \vec{A}_j}{\partial r} + \left[\frac{\omega_j^2}{c^2} - k_j^2 - \frac{\omega_{po}^2}{c^2}\left(1+\frac{r^2}{r_c^2}\right)\right]\vec{A}_j = 0, \tag{3}$$

where $\omega_{po} = (4\pi n_o^o e^2/m)^{1/2}$. Equation (2), for the fundamental modes, gives

$$\begin{aligned} \vec{A}_j &= \vec{A}_{oj} e^{-r^2/2r_o^2}, \\ k_j^2 &= \frac{\omega_j^2 - \omega_{po}^2}{c^2} - \frac{2\omega_{po}}{r_c c}, \\ r_o &= \left(\frac{r_c c}{\omega_{po}}\right)^{1/2}. \end{aligned} \tag{4}$$

The lasers impart oscillatory velocities to electrons,

$$\vec{v}_j = \frac{e\vec{E}_j}{mi\omega_j}, \quad j = 1, 2, \tag{5}$$

and exert a difference frequency ponderomotive force on them:

$$\vec{F}_p = e\nabla\phi_p, \tag{6}$$

where

$$\phi_p = \left(\frac{m}{2e}\right)\vec{v}_1\cdot\vec{v}_2^* = \phi_{po} e^{-r^2/r_o^2} e^{-(\omega t - k' z)} \tag{7}$$

and $\phi_{po} = \frac{eA_{01}A_{02}}{2m\omega_1\omega_2}$, $\omega = \omega_1 - \omega_2$, $k' = k_1 - k_2$. The motion of electrons under the ponderomotive force is governed by the equation of motion

$$m\frac{\partial \vec{v}}{\partial t} = \vec{F}_p - \frac{e}{c}\vec{v}\times\vec{B}_s. \tag{8}$$

Linearizing and solving for $\vec{v}$, one obtains

$$\vec{v}_\perp = \frac{e\nabla\phi_p \times \vec{\omega}_c}{m(\omega^2 - \omega_c^2)} + \frac{i\omega e\nabla_\perp\phi_p}{m(\omega^2-\omega_c^2)}, \quad v_z = -\frac{ek'\phi_p}{m\omega}. \tag{9}$$

This velocity beats with the density ripple to produce a nonlinear current density at $\omega, k'+q$,

$$\vec{J}^{NL} = -\tfrac{1}{2}n'_q e\vec{v} \tag{10}$$

with

$$J_x^{NL} = -\frac{n'_q e^2}{2m(\omega^2-\omega_c^2)}\left[\frac{\partial\phi_p}{\partial y}\omega_c + i\omega\frac{\partial\phi_p}{\partial x}\right], \tag{11}$$

$$J_y^{NL} = \frac{n'_q e^2}{2m(\omega^2-\omega_c^2)}\left[\frac{\partial\phi_p}{\partial x}\omega_c - i\omega\frac{\partial\phi_p}{\partial y}\right]. \tag{12}$$

3. THz generation

The wave equation governing the THz wave field is

$$\nabla^2\vec{E} - \nabla(\nabla\cdot\vec{E}) + \frac{\omega^2}{c^2}\underline{\underline{\varepsilon}}\cdot\vec{E} = -\frac{4\pi i\omega}{c^2}\vec{J}^{NL}, \tag{13}$$

where $\varepsilon_{xx} = \varepsilon_{yy} = 1 - \omega_{po}^2/(\omega^2-\omega_c^2)$, $\varepsilon_{xy} = -\varepsilon_{yx} = i(\omega_c/\omega)\omega_{po}^2/(\omega^2-\omega_c^2)$,

$$\varepsilon_{zz} = 1 - \omega_{po}^2/\omega^2, \varepsilon_{xz} = \varepsilon_{zx} = \varepsilon_{yz} = \varepsilon_{zy} = 0.$$

In principle, the THz wave could have both extraordinary ($E_y = iE_x$) and ordinary ($E_y = -iE_x$) modes but the phase matching condition can be satisfied for only one of them. Following Sodha *et al* [17] we consider the extraordinary mode to be in resonance, i.e. $E_y = iE_x$. Taking $\nabla\cdot$ of equation (13), we have

$$\begin{aligned}\frac{\partial E_z}{\partial z} = &-\frac{1}{\varepsilon_{zz}}\left[\frac{\partial}{\partial x}(\varepsilon_{xx}E_x + \varepsilon_{xy}E_y) + \frac{\partial}{\partial y}(\varepsilon_{xx}E_y - \varepsilon_{xy}E_x)\right] \\ &- \frac{1}{\varepsilon_{zz}}\frac{4\pi i}{\omega}\nabla\cdot\vec{J}^{NL},\end{aligned}$$

which on using $E_y = iE_x$ gives

$$\nabla\cdot\vec{E} = \left(1-\frac{\varepsilon_+}{\varepsilon_{zz}}\right)\left(\frac{\partial E_x}{\partial x} + i\frac{\partial E_x}{\partial y}\right) - \frac{1}{\varepsilon_{zz}}\frac{4\pi i}{\omega}\nabla\cdot\vec{J}^{NL}, \tag{14}$$

where $\varepsilon_+ = \varepsilon_{xx} + i\varepsilon_{xy}$. Ignoring spatial variation in ε_{xx}, ε_{xy}, ε_{zz} (valid for paraxial approximation), using equation (14) in equation (13) we have

$$\begin{aligned}\nabla^2 E_x &- \left(1-\frac{\varepsilon_+}{\varepsilon_{zz}}\right)\frac{\partial^2 E_x}{\partial x^2} - i\left(1-\frac{\varepsilon_+}{\varepsilon_{zz}}\right)\frac{\partial^2 E_x}{\partial x\partial y} \\ &+ \frac{\omega^2}{c^2}(\varepsilon_{xx} + i\varepsilon_{xy})E_x = R_x + \frac{4\pi}{i\omega\varepsilon_{zz}}\frac{\partial}{\partial x}\left(\nabla\cdot\vec{J}^{NL}\right),\end{aligned} \tag{15}$$

$$\begin{aligned}i\nabla^2 E_x &- \left(1-\frac{\varepsilon_+}{\varepsilon_{zz}}\right)\frac{\partial^2 E_x}{\partial x\partial y} - i\left(1-\frac{\varepsilon_+}{\varepsilon_{zz}}\right)\frac{\partial^2 E_x}{\partial y^2} \\ &+ \frac{\omega^2}{c^2}(i\varepsilon_{xx} - \varepsilon_{xy})E_x = R_y + \frac{4\pi}{i\omega\varepsilon_{zz}}\frac{\partial}{\partial y}\left(\nabla\cdot\vec{J}^{NL}\right),\end{aligned} \tag{16}$$

where $\vec{R} = -(\frac{4\pi i\omega}{c^2})\vec{J}^{\rm NL}$. Multiplying equation (16) by i and subtracting from equation (15), one obtains

$$\frac{\partial^2 E_x}{\partial z^2}+\frac{1}{2}\left(1+\frac{\varepsilon_+}{\varepsilon_{zz}}\right)\nabla_\perp^2 E_x+\frac{\omega^2}{c^2}\varepsilon_+ E_x = \frac{1}{2}(R_x - {\rm i}R_y)+\frac{4\pi}{{\rm i}\omega\varepsilon_{zz}}\left(\frac{\partial}{\partial x}-{\rm i}\frac{\partial}{\partial y}\right)\left(\nabla\cdot\vec{J}^{\rm NL}\right), \quad (17)$$

where $\nabla_\perp^2 = \frac{\partial^2}{\partial x^2}+\frac{\partial^2}{\partial y^2}$, $\varepsilon_+ = 1-\frac{\omega_{\rm p}^2}{\omega(\omega-\omega_{\rm c})}$, $\varepsilon_{zz} = 1-\frac{\omega_{\rm po}^2}{\omega^2}$. In the limit $\partial/\partial x, \partial/\partial y \ll k'+q$, the last term in equation (17) can be neglected. In the r-dependent density profile of equation (1), ε_+ can be written as $\varepsilon_{\rm o+}+\varepsilon_{2+}r^2/r_{\rm c}^2$, where $\varepsilon_{\rm o+} = 1-\omega_{\rm po}^2/(\omega(\omega-\omega_{\rm c}))$, $\varepsilon_{2+} = -(\omega_{\rm po}^2/(\omega(\omega-\omega_{\rm c})))$. The $\varepsilon_{2+}r^2/r_{\rm c}^2$ term is more pronounced in equation (17) than elsewhere; hence we write equation (18) as

$$\frac{\partial^2 E_x}{\partial z^2}+\frac{1}{2}\left(1+\frac{\varepsilon_{\rm o+}}{\varepsilon_{zz}}\right)\nabla_\perp^2 E_x+\frac{\omega^2}{c^2}\left(\varepsilon_{\rm o+}+\varepsilon_{2+}\frac{r^2}{r_{\rm c}^2}\right)E_x = \frac{1}{2}\left(\frac{\omega_{\rm po}^2}{c^2}\right)\left(\frac{\phi_{\rm po}r}{r_{\rm o}^2}\right)\left(\frac{\omega}{\omega-\omega_{\rm c}}\right)\left(\frac{n_q}{n_{\rm o}^0}\right)\left(1+\frac{r^2}{r_{\rm c}^2}\right){\rm e}^{-r^2/r_{\rm o}^2}{\rm e}^{-{\rm i}(\omega t-kz+\phi)}, \quad (18)$$

where $k\equiv k'+q$.

Writing

$$E_x = A(r,z){\rm e}^{-{\rm i}(\omega t-kz+\phi)}, \quad (19)$$

equation (18) takes the form

$$2{\rm i}k\frac{\partial A}{\partial z}+\frac{1}{2}\left(1+\frac{\varepsilon_{\rm o+}}{\varepsilon_{zz}}\right)\left(\frac{\partial^2 A}{\partial r^2}+\frac{1}{r}\frac{\partial A}{\partial r}-\frac{A}{r^2}\right) +\left(\frac{\omega^2}{c^2}\varepsilon_{\rm o+}-k^2-\frac{\omega^2}{c^2}\varepsilon_{2+}\frac{r^2}{r_{\rm c}^2}\right)A = G(r), \quad (20)$$

$$G(r) = \frac{1}{2}\left(\frac{\omega_{\rm po}^2}{c^2}\right)\left(\frac{\phi_{\rm po}r}{r_{\rm o}^2}\right)\left(\frac{\omega}{\omega-\omega_{\rm c}}\right)\left(\frac{n_q}{n_{\rm o}^0}\right)\left(1+\frac{r^2}{r_{\rm c}^2}\right){\rm e}^{-r^2/r_{\rm o}^2}.$$

If one ignores the first term on the lhs and takes $G=0$, equation (20) becomes

$$\frac{\partial^2 A}{\partial r^2}+\frac{1}{r}\frac{\partial A}{\partial r}+\left(\alpha_1^2-\frac{1}{r^2}-\frac{r^2}{r_1^4}\right)A = 0, \quad (21)$$

where

$$\alpha_1^2 = 2\left(\frac{\omega^2}{c^2}\varepsilon_{\rm o+}-k^2\right)\bigg/\left(1+\frac{\varepsilon_{\rm o+}}{\varepsilon_{zz}}\right),$$

$$r_1 = \left(-r_{\rm c}^2\frac{c^2}{\omega^2}\left(1+\frac{\varepsilon_{\rm o+}}{\varepsilon_{zz}}\right)/2\varepsilon_{2+}\right)^{1/4}.$$

Writing $\xi = r/r_1$, this equation takes the form

$$\frac{\partial^2 A}{\partial \xi^2}+\frac{1}{\xi}\frac{\partial A}{\partial \xi}+\left(\lambda-\frac{1}{\xi^2}-\xi^2\right)A = 0, \quad (22)$$

where $\lambda = \alpha_1^2 r_1^2$. For the fundamental mode, this equation gives

$$A = \psi(r) = \frac{r}{r_1}{\rm e}^{-r^2/2r_1^2}, \quad (23)$$

with eigenvalue $\lambda = 4$. The phase matching condition requires

$$q = \left[\frac{\omega^2}{c^2}\varepsilon_{\rm o+}-\left(-\frac{8\omega^2\varepsilon_{2+}(1+\varepsilon_{\rm o+}/\varepsilon_{zz})}{c^2 r_{\rm c}^2}\right)^{1/2}\right]^{1/2}-k_1+k_2. \quad (24)$$

When the rhs of equation (20) is finite, we write A as

$$A = F(z)\psi(r), \quad (25)$$

presuming that the eigenfunction remains the same and only amplitude becomes a function of z. Employing equation (25) in equation (20), multiplying the resulting equation by $\psi^* r\,{\rm d}r$ and integrating over r from 0 to ∞, one obtains

$$\frac{\partial F}{\partial z} = -{\rm i}\beta, \quad (26)$$

where

$$\beta = \frac{1}{8}\frac{\omega_{\rm po}^2}{c^2}\frac{\phi_{\rm po}}{r_{\rm o}^2}\frac{\omega}{\omega-\omega_{\rm c}}\left(\frac{r_2^4}{2}+\frac{r_2^6}{r_{\rm c}^2}\right)\frac{1}{kr_1^3}, \qquad r_2 = \frac{1}{(1/2r_1^2+1/r_{\rm o}^2)^{1/2}}.$$

Had one included the collisional damping of the THz wave, equation (26) would take the form

$$\frac{\partial F}{\partial z}+k_i F = -{\rm i}\beta. \quad (27)$$

At large values of z this gives

$$F = -{\rm i}\beta/k_i, \quad (28)$$

where

$$k_i = \frac{\omega_{\rm po}^2\nu}{2c((\omega-\omega_{\rm c})^2+\nu^2)\left(1-\frac{\omega_{\rm po}^2(\omega-\omega_{\rm c})}{\omega((\omega-\omega_{\rm c})^2+\nu^2)}\right)^{1/2}}.$$

So the normalized amplitude of the THz wave is

$$\left|\frac{F}{A_{01}}\right| = \left|\frac{1}{8}\left(\frac{1}{k'k_i'r_1'}\left(\frac{r_2'^4}{2r_1'^2r_{\rm o}'^2}+\frac{r_2'^6}{r_1'^2r_{\rm o}'^2r_{\rm c}'^2}\right)\right)\frac{\omega'}{\omega'-\omega_{\rm c}'}\left(\frac{A_{02}'}{\omega_1'\omega_2'}\right)n_q'\right|, \quad (29)$$

where $A_{02}' = eA_{02}/mc\omega_{\rm po}$, $n_q' = \frac{n_q}{n_{\rm o}^0}$ and all the primed quantities are normalized w.r.t. $\omega_{\rm po}$.

The plot of normalized ripple factor $|qc/\omega_{\rm po}|$ as a function of normalized frequency $|\omega/\omega_{\rm po}|$ is plotted in figure 1. The relevant parameters are $\omega_{\rm c}' = 0.2$, $r_{\rm c}' = 3$, $\nu' = 10$. It is observed that for $\omega_{\rm c}/\omega_{\rm po}\approx 0.2$, the normalized ripple factor decreases steadily from 0.77 to 0.15 as $\omega/\omega_{\rm po}$ is varied from 2 to 10. Also in figure 2 we have plotted the requisite normalized ripple wave number for $\omega_{\rm c}' = 0.2$, 0.6. As the magnetic field increases, the required ripple wave number for phase-matched THz generation rises. In figure 3 we plot normalized THz amplitude as a function of normalized frequency $\omega/\omega_{\rm po}$ for $\omega_1/\omega_{\rm po} = 50\,100$. It is observed that for $\omega_{\rm c}/\omega_{\rm po}\approx 0.2$, the normalized THz amplitude decreases monotonically from 5.56×10^{-4} to 1.5×10^{-4} as $\omega/\omega_{\rm po}$ is varied from 2 to 10 for $\omega_1/\omega_{\rm po} = 50$. In figure 4 for $\omega_{\rm c}/\omega_{\rm po} = 0.2-0.6$, i.e. by increasing the magnetic field, the

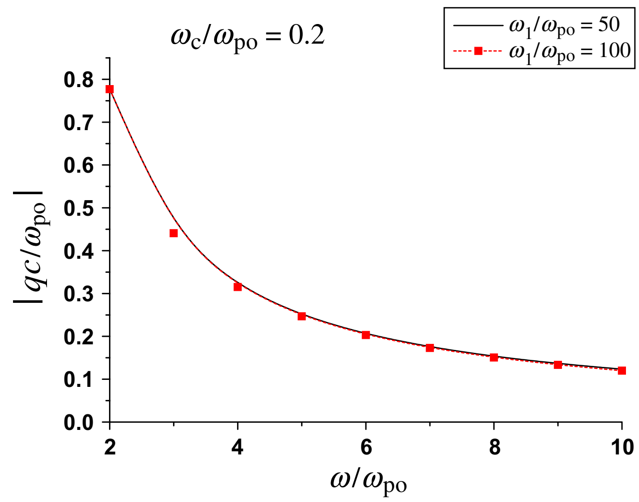

Figure 1. Normalized density ripple wave number $|qc/\omega_{po}|$ as a function of normalized frequency ω/ω_{po} for the value of $\omega_c' = 0.2$, $r_c' = 3$, $\nu' = 10$.

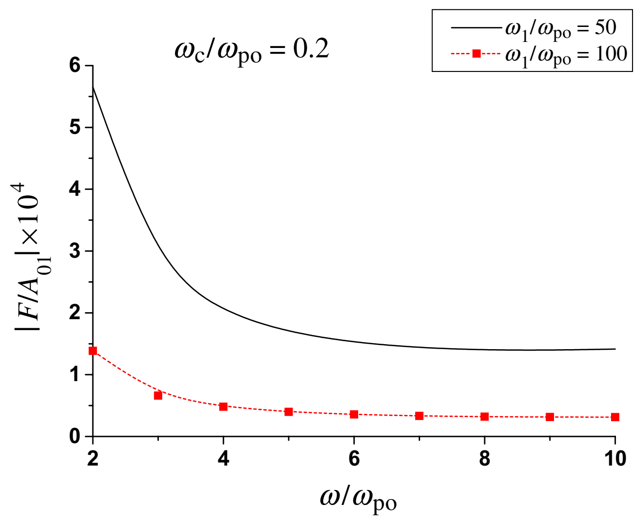

Figure 3. Normalized amplitude of THz radiation $|F/A_{01}|$ as a function of normalized frequency ω/ω_{po} for the value of $A_{02}' = 10$, $r_c' = 3$, $n_q' = 0.3$, $\nu' = 10$.

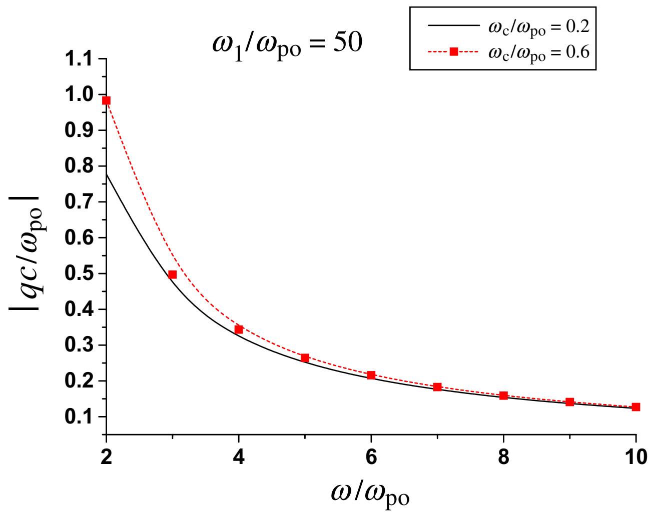

Figure 2. Normalized density ripple wave number $|qc/\omega_{po}|$ as a function of normalized frequency ω/ω_{po} for the value of $\omega_c' = 0.2$, 0.6, $r_c' = 3$, $\nu' = 10$.

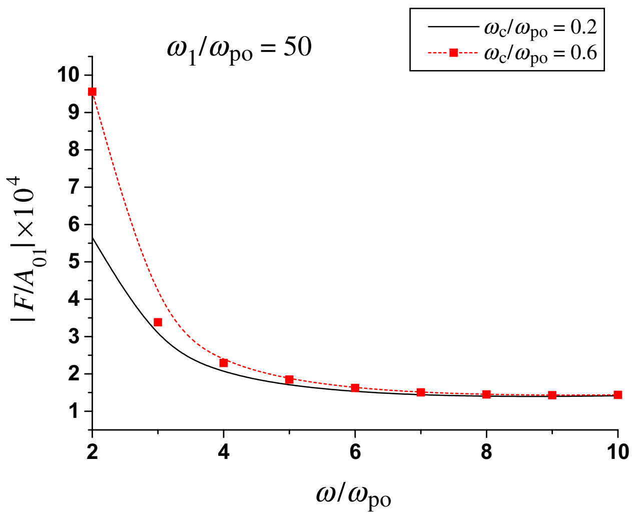

Figure 4. Normalized amplitude of THz radiation $|F/A_{01}|$ as a function of normalized frequency ω/ω_{po} for the value of $\omega_c' = 0.2$, 0.6, $A_{02}' = 10$, $r_c' = 3$, $n_q' = 0.3$, $\nu' = 10$.

normalized THz amplitude rises approximately two-fold at $\omega/\omega_{po} = 2$. These parameters, for $\omega_{po}/2\pi = 1$ THz, $\omega_1 = 3.14 \times 10^{14}$ rad s^{-1} (CO_2 laser), correspond to $B_s = 72$ and 215 kG. The magnetic field could be internally generated or applied externally. A typical magnetic circuit may consist of a current-carrying coil of N turns and a magnetic core of mean length l_c and cross-sectional area A_g. For an iron core with magnetic permeability $\mu_c = 1000$, $l_c = 40$ cm, $A_c = 10^{-2}$ m^{-2}, $l_g \approx 1$ cm, $A_g \approx 10^{-4}$ m^2 and $\mu_g = \mu_o$, a current of 200 A along $N = 1000$ turns produces a magnetic field of 240 kG appropriate to our calculations in this paper.

4. Power of the THz radiation

The power of the THz radiation can be obtained as

$$P_{THz} = \int_0^\infty \frac{c}{4\pi} |F|^2 \eta 2\pi r \, dr, \tag{30}$$

where $\eta = (1 - \frac{\omega_{po}^2}{\omega(\omega-\omega_c)})^{1/2}$ is the refractive index of the magnetized plasma. The normalized power of the THz radiation can be written as

$$\left|\frac{P_{THz}}{P_{Laser}}\right| = \left|\frac{F}{A_{01}}\right|^2 \eta. \tag{31}$$

A plot of the normalized power of THz radiation as a function of normalized frequency is shown in figure 5. It is observed that normalized power also decreases as ω/ω_{po} increases. For $\omega_1/\omega_{po} = 50$, $|P_{THz}/P_{laser}|$ decreases from 2.6×10^{-7} to 0.25×10^{-7} as ω/ω_{po} is varied from 2 to 10, whereas from figure 6 we observed that for $\omega_c/\omega_{po} = 0.2 - 0.6$, i.e. by increasing the magnetic field, the normalized THz power rises approximately three-fold at $\omega/\omega_{po} = 2$.

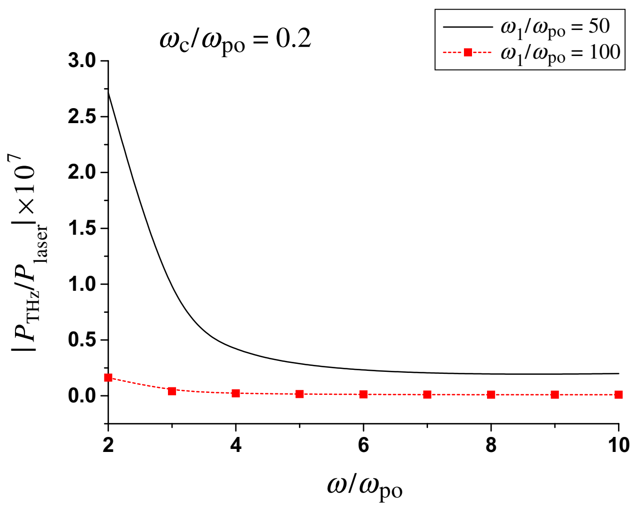

Figure 5. Normalized power of THz radiation $|P_{THz}/P_{laser}|$ as a function of normalized frequency ω/ω_{po} for the value of $A'_{02} = 10$, $r'_c = 3$, $n'_q = 0.3$, $\nu' = 10$.

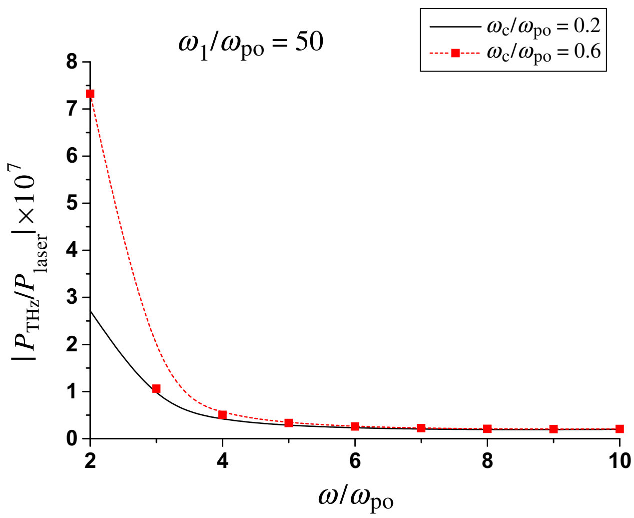

Figure 6. Normalized power of THz radiation $|P_{THz}/P_{laser}|$ as a function of normalized frequency ω/ω_{po} for the value of $\omega'_c = 0.2$, 0.6, $A'_{02} = 10$, $r'_c = 3$, $n'_q = 0.3$, $\nu' = 10$.

5. Discussion

In the present paper, lasers were assumed to be self-guided so that self-focusing was balanced by the diffraction losses. In actual cases, the effect of self-focusing/diffraction can be quite important. One would like to solve the equation governing beam width parameter and incorporate its effect. The pre-existing plasma channel employed here can be created by sending a prepulse of ps durations and allowing substantial time $t' \approx r_c/c_s$, where c_s is the sound speed, before launching the main laser pulses, for plasma to expand under self-pressure gradient via ambipolar diffusion. This requires prepulse intensity $\geqslant 10^{14}\,\mathrm{W\,cm^{-2}}$. Alternatively, one may skip the prepulse and employ the nonlinearities induced by the two main laser beams to create a plasma channel and propagate without self-convergence or divergence. Following Sodha *et al* [17] the condition for self-guiding the two laser beams by offsetting diffraction turns out to be

$$\frac{\omega_{po}^2}{\omega_1^2}\left(\frac{e^2(A_{01}^2+A_{02}^2)}{4m^2\omega_1^2 v_{th}^2}\right)\frac{1}{r_o^2} > \frac{1}{k_1^2 r_o^4}.$$

Acknowledgment

MK is grateful to the Banaras Hindu University, India, for financial support.

References

[1] Pickwell E and Wallace V P 2006 *J. Phys.* D **39** R301
[2] Antonsen T M J, Palastro J and Michberg H M 2007 *Phys. Plasmas* **14** 033107
[3] Shen Y C, Lo T, Taday P F, Cole B E, Tribe W R and Kemp M C 2005 *Appl. Phys. Lett.* **86** 241116
[4] Hamster H, Sullivan A, Gordon S, White W and Falcone R W 1993 *Phys. Rev. Lett.* **71** 2725
[5] Leemans W P *et al* 2003 *Phys. Rev. Lett.* **91** 074802
[6] Schroeder C B, Esarey E, van Tilborg J and Leemans W P 2004 *Phys. Rev.* E **69** 016501
[7] Carr G L, Martin M C, McKinney W R, Jordan K, Neil G R and Williams G P 2002 *Nature* **420** 153
[8] Abo-Bakr M, Feikes J, Holldack K, Kuske P, Peatman W B, Schade U, Wüstefeld G and Hübers H-W 2003 *Phys. Rev. Lett.* **90** 094801
[9] Yoshii J, Lai C H, Katsouleas T, Joshi C and Mori W B 1997 *Phys. Rev. Lett.* **79** 4194
[10] Yugami N, Higashiguchi T, Gao H, Sakai S, Takahashi K, Ito H, Nishida Y and Katsouleas T 2002 *Phys. Rev. Lett.* **89** 065003
[11] Schillinger H and Sauerbrey R 1999 *Appl. Phys. B: Lasers Opt.* **68** 753
Tzortzakis S, Mechain G, Patalano G, Andre Y-B, Parde B, Franco M, Mysyrowicz A, Munier J-M, Gheudin M, Beaudin G and Encrenaz P 2002 *Opt. Lett.* **27** 1944
[12] Mclaughlin R, Corchia A, Johnston M B, Chen Q, Ciesla C M, Arnone D D, Jones G A C, Linfield E H, Davies A G and Pepper M 2000 *Appl. Phys. Lett.* **76** 2038
[13] Liu C S and Tripathi V K 2009 *J. Appl. Phys.* **105** 013313
[14] Pai C-H, Huang S-Y, Kuo C-C, Lin M-W, Wang J, Chen S-Y, Lee C-H and Ylin J 2005 *Phys. Plasmas* **12** 070707
[15] Chien T-Y, Chang C-L, Lee C-H, Lin J-Y, Wang J and Chen S-Y 2005 *Phys. Rev. Lett.* **94** 115003
[16] Layer B D, York A, Antonsen T M J, Verma S, Chen Y H, Leng Y and Milchberg H M 2007 *Phys. Rev. Lett.* **99** 035001
[17] Sodha M S, Ghatak A K and Tripathi V K 1974 *Self-Focussing of Laser Beams in Dielectrics, Plasmas and Semiconductors* (New Delhi: Tata McGraw-Hill)
[18] Gildenburg V B and Vvedenskii N V 2007 *Phys. Rev. Lett.* **98** 245002